JACS
JOURNAL OF THE AMERICAN CHEMICAL SOCIETY
Article
pubs.acs.org/JACS

Concerted Halogen-Bonded Networks with *N*-Alkyl Ammonium Resorcinarene Bromides: From Dimeric Dumbbell to Capsular Architectures

Fangfang Pan, Ngong Kodiah Beyeh,* and Kari Rissanen*

Department of Chemistry, Nanoscience Center, University of Jyvaskyla, P.O. Box. 35, FI-40014 Jyvaskyla yliopisto, Finland

Supporting Information

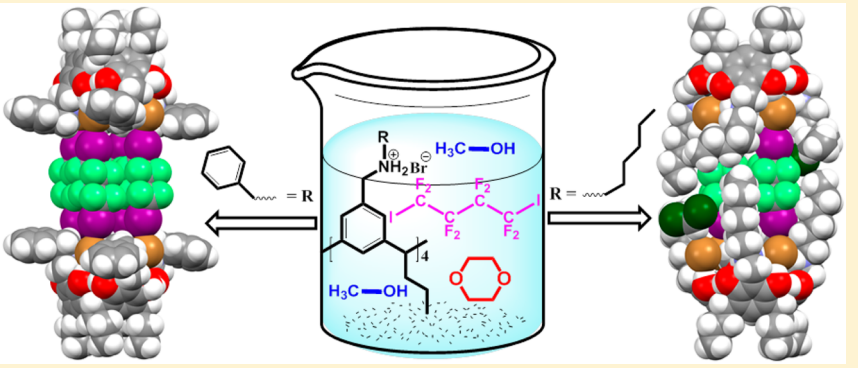

ABSTRACT: *N*-Alkyl ammonium resorcinarene bromides and 1,4-diiodooctafluorobutane via multiple intermolecular halogen bonds (XB) form different exotic supramolecular architectures through subtle changes of the upper rim substituents. Dimeric dumbbell-like assembly with encapsulated guest molecules is generated with *N*-benzyl substituents. The *N*-hexyl groups engender an XB-induced polymeric pseudocapsule and an XB-induced dimeric capsule with entrapped 1,4-dioxane guest molecules. The *N*-propyl and *N*-cyclohexyl groups generate deep cavity cavitands. The deep cavity cavitands possess cavities for self-inclusion leading to polymeric herringbone arrangement in one direction and that pack into 3D polymeric arrangement resembling egg crate-like supramolecular networks. These assemblies are studied in solution via NMR spectroscopy and in the solid state via X-ray crystallography.

1. INTRODUCTION

The utilization of weak interactions in the design of functional assemblies is a challenge, from both fundamental and application purposes.[1] Anions adopt multiple coordination geometries and can participate in noncovalent interactions such as electrostatics, metal coordination, anion−π, and hydrogen bonding.[2] The hydrogen bond (HB) is arguably the most frequently used weak interaction in the design of organic supramolecular architectures.[3] Halogen bonding (XB) resulting from the noncovalent interaction between polarized halogen atoms and Lewis bases was recently defined[4] and has been demonstrated to show efficient directional interactions with anions. The halogens in XB donors have been shown to exhibit an anisotropic electron distribution resulting in an electropositive region on the halogen commonly named as the σ-hole.[5] The strongest XB interactions (A-Hal···X^-) are observed with the most polarizable halogens in the order I > Br ≫ Cl ≫ F.[6]

Anions being good Lewis bases have been shown to be suitable HB and XB acceptors.[4,6,7] The spherical, symmetrical, and electronic nature of halides makes them excellent electron donors as the negative charge is concentrated on a single atom.[6,7] By virtue of these properties, halides can adopt numerous coordination numbers.[8] The cooperative utilization of both HB and XB to form distinct functional assemblies is rare, and when it does occur, a compromise between the distinct preferences of the two interactions is observed.[9] Anions have templated multiple supramolecular networks with various XB donors.[10] Ditopic, tritopic, and tetratopic XB donors with the association of different halide anions afford interesting 2D and 3D structures.[11] These structures include tubular assemblies and honeycomb and corrugated networks.[11] The two-fold interpenetrated, pyrite-type, cubic lattices with octahedral coordination around the halide anion are also reported.[12]

The *N*-alkyl ammonium resorcinarene halides (NARXs) are formed through the cleavage of tetrabenzoxazines by hydrogen halides under refluxing conditions.[13] The halide anions and the $-NH_2^+-R$ moieties through very strong intramolecular HBs form a circular cation−anion seam resembling extended cavitand-like structures.[13] Chlorides and bromides are optimum anions for this process by virtue of their size and electronic and HB acceptor affinity.[13] These large organic salt molecules

Received: June 25, 2015
Published: July 27, 2015

DOI: 10.1021/jacs.5b06590
J. Am. Chem. Soc. 2015, 137, 10406−10413

possessing concave cavities are versatile receptors that can be used to bind a variety of guests through a series of weak interactions. The halides of the NARXs are suitable for XB interactions with suitable XB donors, thus extending the preorganized cavities of these assemblies under certain conditions,[14] which therefore expand their application in guest recognition.

The NARXs are specific intramolecular salts where the four ammonium cations and four anions are embedded into a single resorcinarene skeleton.[13] They are therefore single molecules with four possible XB binding sites (the four anions). The resorcinarene frame and the HB interactions with the ammonium ions block part of the coordination sphere of the halides in these multivalent systems so that in the presence of suitable XB donors, XB interactions can only occur either from the upper rim of the resorcinarenes or from the side while preserving the interior cavity of these receptors for guest binding.[14] This contributes to the rational design of the halogen-bonded supramolecular assemblies. The XB donors can be inorganic or organic, which result in XBs of different nature. The former which involves inorganic donors is usually regarded to be dominated by charge transfer interaction, while electrostatic force is mainly responsible for the latter type. Just recently, we successfully constructed the halogen-bonded capsule from *N*-cyclohexyl ammonium resorcinarene chloride and elemental I_2, which possesses enough space in the cavity to encapsulate three ordered 1,4-dioxane molecules occupying 55.2% of the confined space, thus respecting the Rebek[15] 55% rule.[16]

While single crystal X-ray diffraction has become one of the main tools in the investigation of XB interactions,[6,8,11,12,17] demonstrating XB in solution is a tedious and sometimes an elusive process due to solvent interference. However, NMR spectroscopy has been shown to be a powerful and often reliable tool to study XB in solution.[18] In this contribution, we report the formation of several XB assemblies utilizing several *N*-alkyl ammonium resorcinarene bromides (NARBrs) **1**−**4** as XB acceptors and 1,4-diiodooctafluorobutane **5** as the XB donor (Figure 1). Subtle changes of the upper rim substituents led to quite different exotic supramolecular structures while preserving the cavity for guest binding. The *N*-benzyl NARBr **1** and four 1,4-diiodooctafluorobutane **5** formed a dimeric dumbbell assembly through eight intermolecular XBs. The binding of small guests such as 1,4-dioxane **6** and *N*-methylacetamide **7** in the resorcinarene cavity is observed in the presence of the XB donor. Changing the upper rim to *N*-hexyl analogue **2** gave an XB-induced polymeric resorcinarene bromide pseudocapsule and an XB-induced dimeric resorcinarene capsule, while *N*-propyl and *N*-cyclohexyl groups **3** and **4** engendered deep cavity cavitands with interesting binding and packing properties.

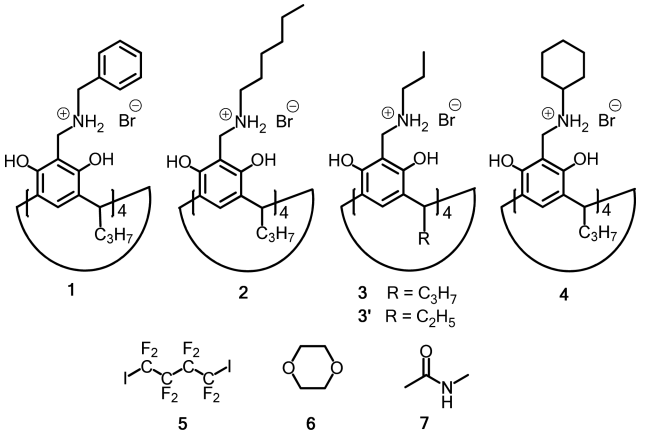

Figure 1. Representative of tetravalent XB acceptors, NARBrs **1**−**4**, XB donor **5**, and guests **6** and **7**.

2. RESULTS AND DISCUSSION

Mannich condensation reaction between aliphatic amines and resorcinarenes in the presence of excess formaldehyde results in tetrabenzoxazines.[13] Ring opening of the six-membered tetrabenzoxazine ring in the presence of hydrobromic acid under refluxing conditions gives NARBrs **1**−**4** (Figure 1) in reasonable yields.[13] The HBs between the ammonium moieties and the bromides form a strong circular HB seam $(\cdots NArRH_2^+\cdots Br^-\cdots NArRH_2^+\cdots Br^-\cdots)_2$ possessing a cavity size and shape analogous to covalent resorcinarene cavitands.[13]

2.1. Dimeric Dumbbell Assembly. *2.1.1. NMR Spectroscopy.* Despite the difficulty in demonstrating XB in solution due to solvent interference, reports show NMR spectroscopy to be the most powerful and reliable tool to study XB in solution.[18] Perfluorohalocarbons (PFHC) are widely studied XB donors and are considered to be "iconic" XB donors.[6,8−12] However, reports of the utilization of PFHC in the construction of XB assemblies involving preorganized concave molecular entities are sparse.[14b,19] Diederich and co-workers[20] recently reported a cavitand-based halogen-bonded heterocapsule with guest binding properties in solution. We recently reported the solid-state structure of halogen-bonded analogues of deep cavity cavitands involving the NARCls.[14] The bromide anions of the NARBrs are hydrogen bonded to the ammonium and the hydroxyl groups. If they are also involved in XB in a synergistic manner, changes in the ^{1}H NMR chemical shifts of the −OH and $-NH_2$ protons of the NARBr hosts **1**−**4** that are hydrogen bonded to the bromides anions are expected. Therefore, the ^{1}H, ^{19}F, and ^{13}C NMR spectroscopies were utilized to study the possible XB assemblies formed between the NARBrs **1**−**4** and 1,4-diiodooctafluorobutane **5** in solution.

The NARXs are known to bind small guest molecules such as 1,4-dioxane and low molecular weight alcohols.[13] Recent reports also showed these host compounds to bind mono- and diamides with cooperativity in chloroform.[21] A series of ^{1}H NMR measurements was performed in a mixture of $CDCl_3$/CCl_4 (1:1 v/v) to investigate the existence of XB in solution and to probe the host−guest properties of the assemblies. Pure CCl_4 could not be used due to limited solubility of the NARBrs. Several samples (10 mM), containing the *N*-benzyl NARBr **1**, the XB donor **5** in 1:2 ratio, and/or with slight excess of the guest molecules **6** and **7**, were prepared, and their NMRs recorded at 303 K. ^{1}H NMR showed changes in the −OH and $-NH_2$ signals of the NARBr **1** attributed to the formation of XB in solution (Figures 2I and S1). In the presence of guests **6** and **7**, ^{1}H NMR reveals significant complexation-induced shielding of the guest protons from samples $\mathbf{1}\cdot\mathbf{5}_2\cdot\mathbf{6}$ and $\mathbf{1}\cdot\mathbf{5}_2\cdot\mathbf{7}$, where the numbers in bold represent the compounds and the subscript(s) indicate the corresponding ratio, thus $\mathbf{1}\cdot\mathbf{5}_2\cdot\mathbf{6}$ indicates that the assembly consists of one molecule of **1**, two molecules of **5** (as a capsule), and one molecule of **6**. The complexation-induced ^{1}H NMR shifts of the guest protons, changes in the hosts −OH and the $-NH_2$ protons were observed from the samples containing the host **1**, XB donor **5**, and the guests **6** and **7**, (Figures 2 and S2), thus supporting the

DOI: 10.1021/jacs.5b06590
J. Am. Chem. Soc. 2015, 137, 10406−10413

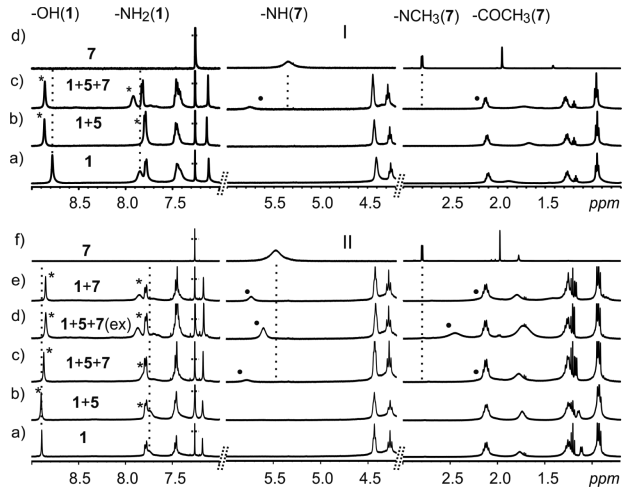

Figure 2. (I) ^{1}H NMR in $CDCl_3/CCl_4$ (1:1 v/v) at 303 K of: (a) **1** (10 mM), (b) 1:2 mixture of **1** and **5**, (c) 1:2:1 mixture of **1**, **5**, and **7**, and (d) **7** (10 mM). (II) ^{1}H NMR in $CDCl_3$ at 303 K of: (a) **1**, (b) 1:2 mixture of **1** and **5**, (c) 1:2:1 mixture of **1**, **5**, and **7**, (d) 1:2:excess mixture of **1**, **5**, and **7**, (e) 1:1 mixture of **1** and **7**, and (f) **7** (10 mM). Stars indicate shifts resulting from the formation of either XBs and/or guest binding. Black dots indicate complexation induced shielding of the guest **7**.

existence of HB and XB in solution with guest binding properties.

The chloroform hydrogen atom is acidic enough to interfere with weak interactions such as HB and XB when in bulk amounts. This effect was confirmed when comparing the spectra measured in pure $CDCl_3$ to that measured in $CCl_4/CDCl_3$ (1:1 v/v) mixture. Though changes in the −OH and $-NH_2$ ^{1}H NMR signals of the host and the guests signals support the existence of XB in pure $CDCl_3$, the chemical shifts were smaller than those observed in $CCl_4/CDCl_3$ mixture (for example: **1**·$\mathbf{5}_2$: in $CDCl_3$, −OH 0.00 ppm and $-NH_2$ −0.01 ppm; in $CCl_4/CDCl_3$, −OH +0.08 ppm and $-NH_2$ −0.05 ppm). This phenomenon was also apparent in the presence of the guests (for example: **1**·$\mathbf{5}_2$·**7**; in $CDCl_3$, −NH of **7**, +0.31 ppm, −OH, −0.02 ppm and $-NH_2$, +0.06 ppm; in $CCl_4/CDCl_3$, −NH of **7**, +0.41 ppm, −OH, +0.08 ppm and $-NH_2$, +0.07 ppm, Figure 2). These results thus confirm the apparent interference of the bulk $CDCl_3$.

^{19}F NMR experiments in $CDCl_3$ at 303 K were done to further probe the existence of the halogen-bonded assemblies in solution. In the analyses, the fluorine signals of the XB donor **5** were monitored. Minor upfield shifts of the fluorine atoms attached to the same carbon atom as the iodines were observed (0.08 ppm in **1**·$\mathbf{5}_4$, 0.06 ppm in **1**·$\mathbf{5}_4$·**6**, and 0.06 ppm in **1**·$\mathbf{5}_4$·**7**, Figure 3), thus confirming the results observed via the ^{1}H NMR experiments.

Despite the low sensitivity of ^{13}C NMR, several measurements were done to further probe the guest binding properties of the HB and XB assemblies. Samples containing various mixtures of the *N*-benzyl NARBr **1**, the XB donor **5**, and the guests **6** and **7** were prepared, and the ^{13}C NMR measurements performed with results clearly confirming guests binding in solution (Figures 4 and S3).

The stoichiometry of the XB assembly between the *N*-benzyl NARBr **1** and the XB donor **5** was investigated in solution through Job plot experiments following the $-NH_2$ signals of NARBr **1**.[22] Job plot experiments have a general limitation on

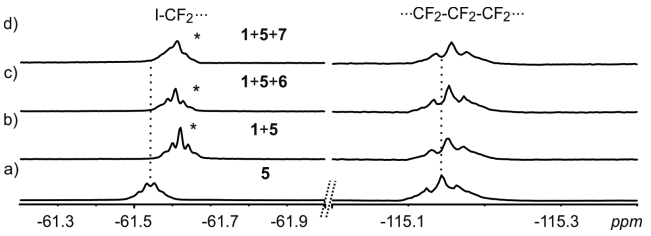

Figure 3. ^{19}F NMR in $CDCl_3$ at 303 K of: (a) **5** (10 mM), (b) 1:2 mixture of **1** and **5**, (c) 1:2:1 mixture of **1**, **5** ,and **6**, and (d) 1:2:1 mixture of **1**, **5**, and **7**. Stars indicate shifts resulting from the formation of XBs.

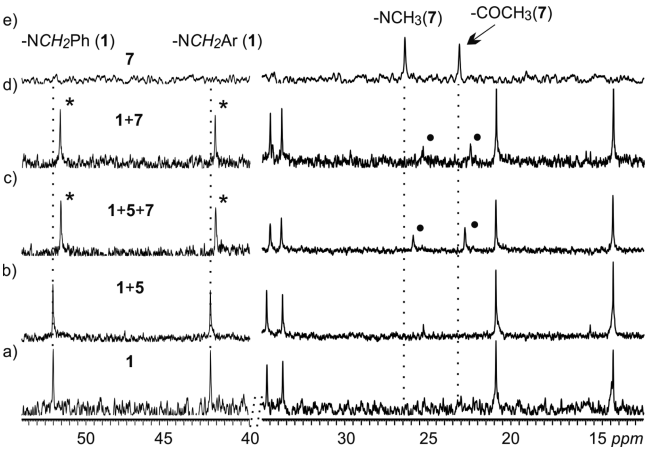

Figure 4. ^{13}C NMR in $CDCl_3$ at 303 K of: (a) **1** (10 mM), (b) 1:2 mixture of **1** and **5**, (c) 1:2:1 mixture of **1**, **5**, and **7**, (d) 1:1 mixture of **1** and **7**, and (e) **7** (10 mM). Stars indicate shifts resulting from the formation of either XBs and/or guest binding. Black dots indicate complexation induced shielding of the guest **7**.

complex systems other than a 1:1 stoichiometry.[22c] The Job plot did not show a predominant species in solution with the maximum at 0.6. The ^{1}H and ^{19}F NMR spectra shifts clearly support the halogen bonding in solution, therefore the Job plot can be interpreted as showing a very dynamic mixture of variants of 1:1 and 1:2 (2:4) XB assemblies (Figure 5).

2.1.2. X-ray Crystallography. The XB interactions between the resorcinarene host **1** and the XB donor **5** have been clearly detected in solution by NMR spectroscopy. However, it is difficult to model the exact supramolecular assemblies from the

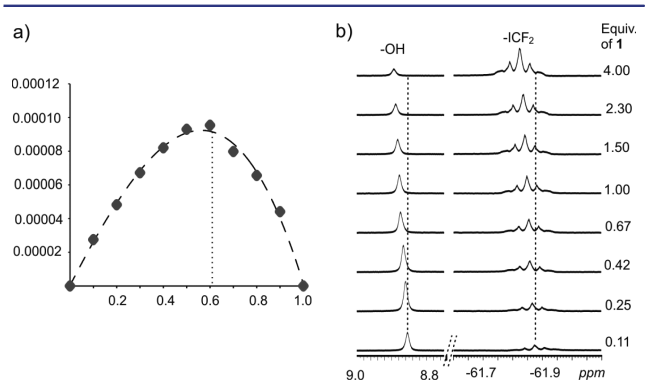

Figure 5. (a) Job plot from a mixture of **1** and **5** in $CDCl_3$ at 303 K depicting a dynamic mixture of variants of 1:1 and 1:2. (b) ^{1}H and ^{19}F NMR spectra changes from the Job plot.

DOI: 10.1021/jacs.5b06590
J. Am. Chem. Soc. 2015, 137, 10406−10413

results. Therefore, single crystal X-ray diffraction was utilized to study the formed assemblies in the solid state.

Crystallization of the *N*-benzyl NARBr **1** with slight excess of the XB donor **5** and 1,4-dioxane in chloroform resulted in single crystals corresponding to the assembly [(**6**@**1**)·$\mathbf{5}_5$·(**6**@**1**)] (Figure 6). The molecules aggregate in a triclinic *P*-1 space

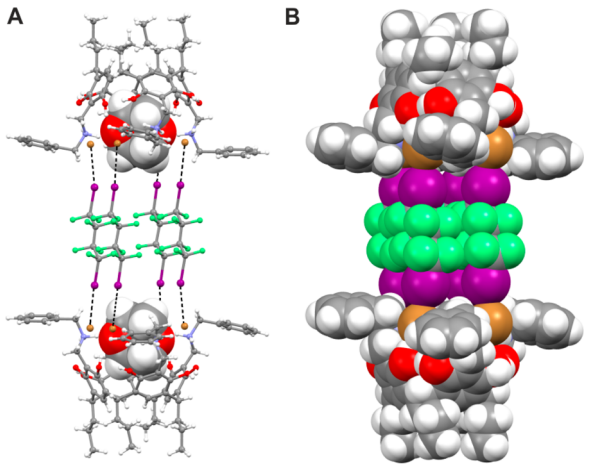

Figure 6. Halogen-bonded NARBr **1** forming a dimeric dumbbell assembly: (A) Ball-and-stick model with the in-cavity 1,4-dioxane in CPK mode and (B) CPK mode to show the dumbbell shape.

group, with the unit cell containing a "dumbbell"-shaped XB dimer with entrapped 1,4-dioxane and out-of-cavity 1,4-dioxane molecules (Figures 6 and S7A). Intramolecular −OH···Br and/or $-NH_2$···Br HBs hold the Br^- anions on the edge of the resorcinarene seam, and four XB donor **5** links two of the resorcinarene salt molecules with Br···I XBs, forming the "dumbbell-shaped" dimeric assembly. The fifth XB donor **5** molecule interacts with one of the bromide anions by XB, providing the additional extension of the dimer along crystallographic [0 1 1] direction leading to a 1D polymer of dimers (Figure 7A). The benzyl groups on the host **1** in the 1D polymers $\pi\cdots\pi$ stack with each other, extending the assembly into a 2D network in (0 1 1) plane (Figure 7B). Along the [0 1 $\bar{1}$] direction, intermolecular −OH···Br HBs connect the resorcinarene cations, thus generating a 3D XB−HB network (Figure 7C). The distances of Br···I XBs range from 3.306 to 3.382 Å less than the average value (3.480 Å) found from 142 published error/disorder-free single crystal structures containing Br···I contacts in the Cambridge Structural Database (CSD version 5.36, November 2014).[23] The halogen-bonding ratio R_{XB} ($R_{XB} = d_{XB}/(X_{vdW} + B_{vdW})$) can be used to roughly measure the strength of the XB interactions.[24] In this "dumbbell" the R_{XB} ranges from 0.86 to 0.88. It is worth noting that the four XB donors **5** that dimerize the NARBr **1** interact with each other through fluorine−fluorine interactions,[25] blocking the potential inside space for guest molecules. It therefore prevents the possibility of a single cavity dimeric capsule formation. However, this XB dimeric assembly highlights the possibility of utilizing concave multivalent systems to construct purely organic halogen-bonded dimeric capsules.

2.2. XB-Induced Polymeric Pseudocapsule and Dimeric Capsule. *2.2.1. NMR Spectroscopy.* As is the case with NARBr **1**, a series of NMR measurements in $CDCl_3$ at 303 K were done to investigate the existence of XB in solution with the *N*-hexyl NARBr **2** and subsequently study their host guest properties. Several samples containing the resorcinarene host **2**,

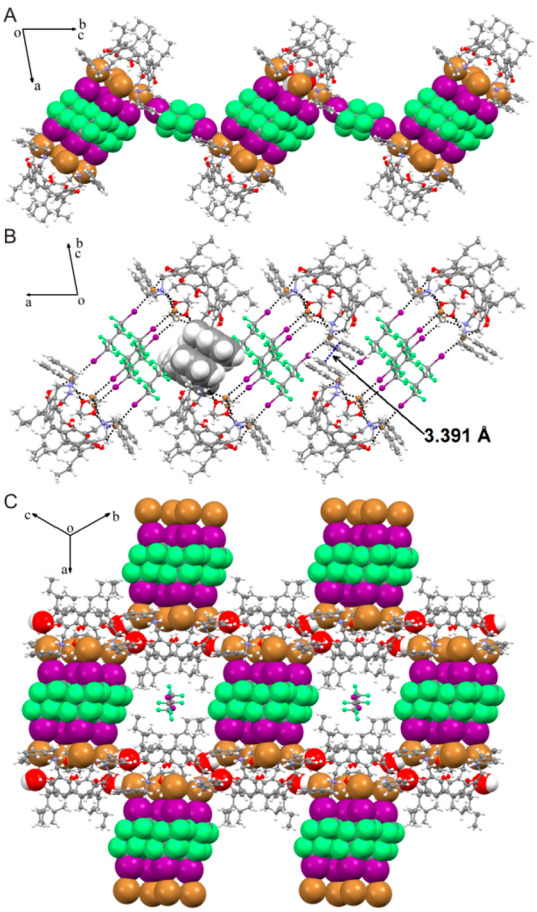

Figure 7. Packing of the assembly [(**6**@**1**)·$\mathbf{5}_5$·(**6**@**1**)]: (A) the halogen-bonded 1D chain; (B) the $\pi\cdots\pi$ interactions between the XB chains, highlighted in CPK, with the shortest C−C distance of 3.391 Å; and (C) the hydrogen bonding between the dumbbells with the species involved in HBs and XBs in CPK mode.

the XB donor **5**, and the guest molecules **6** and **7** in 1:2:1 ratios were prepared and their NMRs were recorded. ^{1}H NMR showed small changes in the −OH and $-NH_2$ signals of the host **2** attributed to the formation of XB in solution (Figures 8 and S4). Significant complexation-induced shielding of the ^{1}H NMR resonances of the guest protons was observed in the presence of guests **6** and **7**, from samples **2**·$\mathbf{5}_2$·**6** and **2**·$\mathbf{5}_2$·**7**.

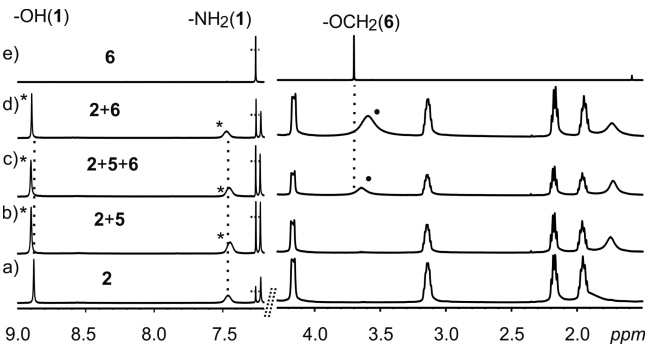

Figure 8. ^{1}H NMR in $CDCl_3$ at 303 K of: (a) **2** (10 mM), (b) 1:2 mixture of **2** and **5**, (c) 1:2:1 mixture of **2**, **5**, and **6**, (d) 1:1 mixture of **2** and **6**, (e) **6** (10 mM). Stars indicate shifts resulting from the formation of XBs, and black dots indicate complexation induced shielding of the guest **6**.

DOI: 10.1021/jacs.5b06590
J. Am. Chem. Soc. 2015, 137, 10406−10413

These complexation-induced ^{1}H NMR shifts of the guest protons, the changes in the hosts −OH and $-NH_2$ protons observed from the samples containing the host **2**, XB donor **5**, and the guests **6** and **7**, (Figures 8 and S4) thus support the existence of HB and XB in solution with guest binding properties. A closer look at the ^{1}H NMR reveals the influence of the protons based on XB is countered by the opposite effect of guest encapsulation. Taking the host $-NH_2$ signal as an example, in the presence of the XB donor **2**·$\mathbf{5}_2$, upfield shift is observed. The same host in the presence of the guest **2**·**6**, downfield sifts of the $-NH_2$ signal is observed. In the presence of both the XB donor and the guest **2**·$\mathbf{5}_2$·**6**, the $-NH_2$ signal is located in the middle thus highlighting the opposite effects of the weak interactions (Figure 8). Similar effects were seen with the guest **7** (Figure S4). These results are comparable with the results seen with the host **1**.

Additionally, ^{19}F NMR experiments in $CDCl_3$ at 303 K were done to further support the existence of the XB assemblies in solution. Minor upfield shifts of 0.07 ppm of the fluorine atoms attached to the same carbon atom as the iodines were observed (Figure 9). ^{13}C NMR experiments were also performed to

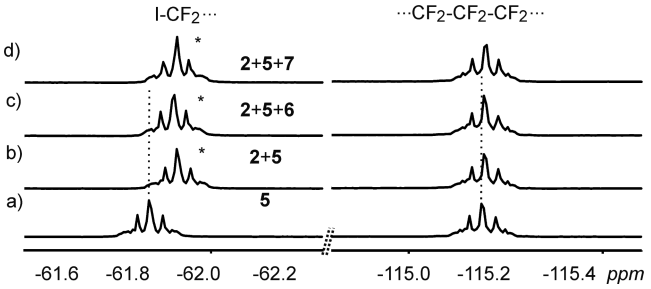

Figure 9. ^{19}F NMR in $CDCl_3$ at 303 K of: (a) **5** (10 mM), (b) 1:2 mixture of **2** and **5**, (c) 1:2:1 mixture of **2**, **5**, and **6**, and (d) 1:2:1 mixture of **2**, **5**, and **7**. Stars indicate shifts resulting from the formation of XBs.

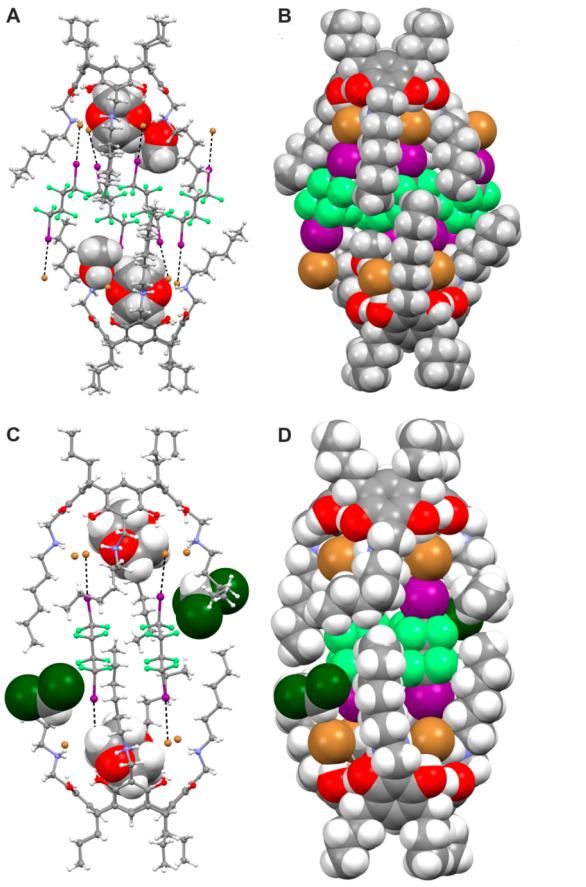

Figure 10. NARBr **2** forming a 1D XB pseudocapsular polymeric [(**6**$_{1.5}$·MeOH@**2**)·$\mathbf{5}_3$·(**6**$_{1.5}$·MeOH@**2**)]$_n$ (A and B) and an XB dimeric capsule [(**6**·$CHCl_3$@**2**)·$\mathbf{5}_2$·(**6**·$CHCl_3$@**2**)] (C and D): view of ball-and-stick mode with the in-cavity 1,4-dioxane and solvent molecules in CPK (A and C); CPK model to highlight the capsular complex (B and D).

further confirm the guest binding properties of the HB and XB assemblies, and the results thus prove guests binding in solution (Figures S5 and S6).

2.2.2. X-ray Crystallography. The methylene spacers in the upper rim of benzyl groups are responsible for the conformational twisting and $\pi\cdots\pi$ stacking with the phenyl rings oriented parallel to the cation−anion seam. Changing the upper rim of the NARBr from *N*-benzyl to *N*-hexyl groups removes the conformational twisting and $\pi\cdots\pi$ stacking. Crystallization of *N*-hexyl NARBr **2** with 4 equiv of the XB donor **5** in the presence of 1,4-dioxane in methanol or chloroform resulted in suitable single crystals corresponding to the assemblies [(**6**$_{1.5}$·MeOH@**2**)·$\mathbf{5}_3$·(**6**$_{1.5}$·MeOH@**2**)]$_n$ (Figure 10A,B) and [(**6**·$CHCl_3$@**2**)·$\mathbf{5}_2$·(**6**·$CHCl_3$@**2**)] (Figure 10C,D), respectively.

In methanol, the molecules aggregate in space group *P*-1 with the unit cell containing a halogen-bonded NARBr **2** dimer and 1,4-dioxane molecules entrapped in each host cavity and outside the cavity between the propyl tails (Figure S7B). As with the "dumbbell" assembly, the four Br^- anions in this structure are also situated in the HB seam involving the intramolecular −OH···Br and/or $-NH_2\cdots$Br interactions. Although excess of the XB donor was used for the crystallization, the compositional ratio of the host, guest (1,4-dioxane), and XB donor in the structure is 2:4:3. In other words, only three of the four Br^- anions in each host molecule are involved in XBs, while the fourth Br^- donates electrons to a methanol molecule, which is located between the two *N*-hexyl arms (Figure 10A,B). As shown in Figure 10A,B, the *N*-hexyl NARBr **2** dimerizes by two XB donor **5**, with the other two stretching outside the dimer toward the neighbors, correspondingly extending the structure into a 1D XB polymer along crystallographic *a* axis direction (Figure 11A,B).

The *N*-hexyl NARBr **2** molecules along *a* axis direction pack into a tube, with the XB donors somewhat located within the capsule. In this respect, packing of the resorcinarene salts along this direction can be considered as a XB induced polymeric capsule. Interestingly, the channel of the capsule is rich in fluorine−fluorine contacts similar to that observed in the "dumbbell" assembly. Along *b* direction, OH···Br HBs connect the 1D XB polymers, thus a 2D network in *ab* plane is formed by the tandem of HBs and XBs (Figure 11). The van der Waals interactions are mainly responsible for the molecular packing along the third direction. The three independent Br···I halogen-bonding distances in this structure are 3.265, 3.355, and 3.410 Å with R_{XB} ratio of 0.85, 0.88, and 0.89, respectively. Again, compared with the average Br···I length found from the CSD,[22] the XB interactions in this architecture are reasonably strong.

In chloroform, a resorcinarene dimer is detected (Figure 10C,D). Even less XB donor molecules **5** participate in the molecular construction, with the host, guest (1,4-dioxane), and XB donor ratio of 2:2:2. In addition to the difference that one $CHCl_3$ molecule replaces the MeOH, the supramolecular

DOI: 10.1021/jacs.5b06590
J. Am. Chem. Soc. 2015, 137, 10406−10413

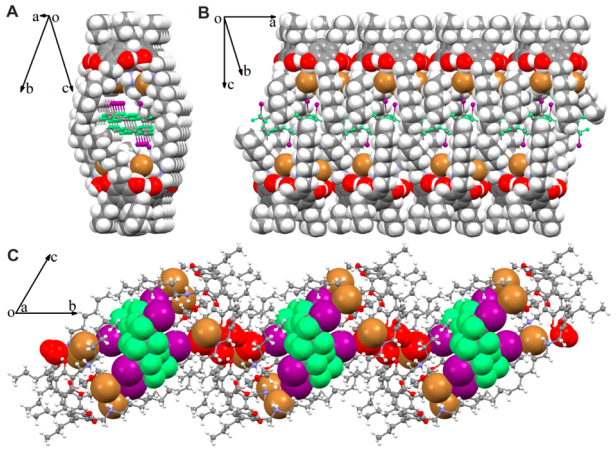

Figure 11. View of the 1D pseudocapsular polymer $[(\mathbf{6}_{1.5}\cdot MeOH@\mathbf{2})\cdot\mathbf{5}_3\cdot(\mathbf{6}_{1.5}\cdot MeOH@\mathbf{2})]_n$ to show the cavity encapsulating the XB donor **5** (A) and the packing along *a* direction (B) as well as the intermolecular HBs along the *b* direction (C).

assembly in this structure is also different. In the assembly $[(\mathbf{6}_{1.5}\cdot MeOH@\mathbf{2})\cdot\mathbf{5}_3\cdot(\mathbf{6}_{1.5}\cdot MeOH@\mathbf{2})]_n$, the two *N*-hexyl ammonium resorcinarene molecules forming XB-induced pseudodimer are arranged in a staggered manner, while in the structure $[(\mathbf{6}\cdot CHCl_3@\mathbf{2})\cdot\mathbf{5}_2\cdot(\mathbf{6}\cdot CHCl_3@\mathbf{2})]$, the dimer consists of two head-to-head eclipsed NARBr **2** molecules with a pseudocenter of inversion, for which reason, the long arms of the *N*-hexyl NARBr **2** are twisted in a different way. Two adjacent Br^- anions of each NARBr **2** molecule are involved in halogen-bonding dimerization in the chloroform assembly, while the two dimerizing Br^- are in opposite positions in the MeOH assembly. However, in both cases, the connecting XB donors are encapsulated inside the NARBr **2** cavities together with two 1,4-dioxane molecules, while the head-to-head arrangement of the resorcinarene creates some space in the wall of the XB-induced resorcinarene capsule (Figure 10D). Interdimeric HBs between two adjacent resorcinarene along [1 1 1] direction (Figure 12A) and lone-pair···π contacts between $CHCl_3$ molecules and phenyl rings of the resorcinarene frame along [1 1 $\bar{1}$] direction (Figure 12B) play important roles in the

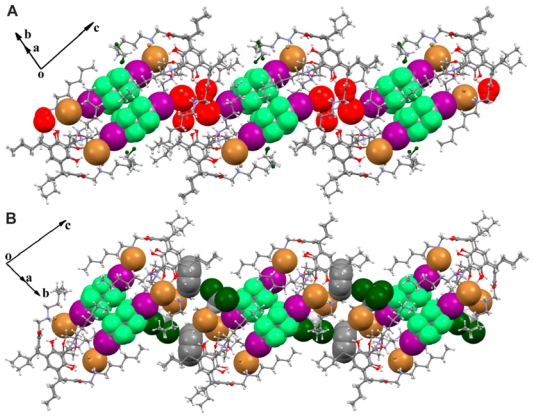

Figure 12. View of the 1D connections of the XB dimers $[(\mathbf{6}\cdot CHCl_3@\mathbf{2})\cdot\mathbf{5}_2\cdot(\mathbf{6}\cdot CHCl_3@\mathbf{2})]$ via OH···Br HBs along [1 1 1] direction (A), and lone pair···π interactions between $CHCl_3$ and phenyl ring of the resorcinarene along [1 1 $\bar{1}$] direction (B). To highlight the relevant interactions, the HBs in A are shown with CPK in red, and the lone-pair···π in B is represented in CPK type.

extension of the structure and work together generating a 2D network in (1 1 0) plane. Additionally, weaker OH···O HBs (actually bifurcated HB) participate in the 3D network formation along the third direction (Figure S8). The Br···I XB interactions in this structure are comparable with those in the XB "dumbbell" and polymer assemblies, showing very narrow range of distances from 3.305 to 3.367 Å and R_{XB} from 0.86 to 0.88.

2.3. Deep Cavity Cavitands. *2.3.1. NMR Spectroscopy.* After exploring the different HB and XB assemblies with *N*-benzyl and *N*-hexyl groups, we then proceeded to explore the possible assembly with short *N*-propyl and rigid *N*-cyclohexyl upper rim substituents. Unfortunately, the low solubility of the *N*-propyl NARBrs **3** in $CDCl_3$ at concentrations above 10 mM prevented the solution investigation and the direct comparison with the *N*-benzyl and the *N*-hexyl groups. However, ^1H NMR measurements at the 5 mM concentration range were done with samples containing the host **3**, the XB donor **5**, and the guest **7** in $CDCl_3$ at 303 K (Figure 13). Despite the low

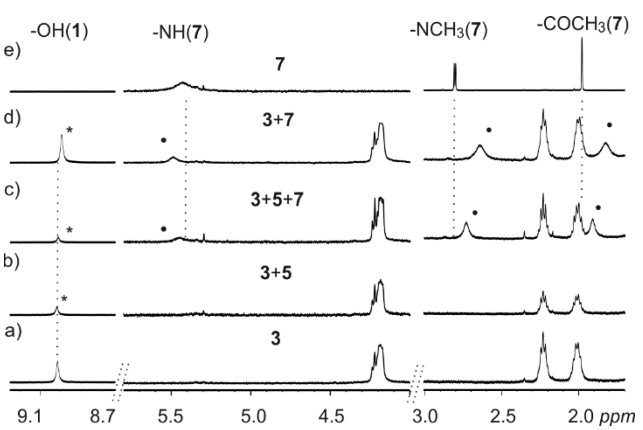

Figure 13. ^1H NMR in $CDCl_3$ at 303 K of: (a) **3** (5 mM), (b) 1:4 mixture of **3** and **5**, (c) 1:4:1 mixture of **3**, **5**, and **7**, (d) 1:1 mixture of **3** and **7**, (e) **7** (5 mM). Black dots indicate complexation induced shielding of the guest **7**.

concentration, ^1H NMR shows guest encapsulation of the assembly resembling the changes seen with the host **1** and **2**. The −OH and $-NH_2$ signals of the host of the sample containing only the host and the XB donor did not show any real changes as was the case with host **1** and **2** (Figure 13). The ^{19}F NMR also did not show any real change. This result also highlights the sensitivity of XB to concentration in solution.[14b]

2.3.2. X-ray Crystallography. In the crystallization experiments, both *N*-propyl NARBrs **3** (Figures 14 and S9A) and **3′** (Figure S9B) and *N*-cyclohexyl NARBr **4** (Figure S9C) crystallize with XB donor **5** in methanol in the presence of 1,4-dioxane, resulting in structures of the same packing, although the assembly $[(\mathbf{6}_2@\mathbf{3})\cdot\mathbf{5}_2]$ crystallizes in orthorhombic space group *Ccce*, while $[(\mathbf{6}_2@\mathbf{3}')\cdot\mathbf{5}_2]$ and $[(\mathbf{6}_2@\mathbf{4})\cdot\mathbf{5}_2]$ are in tetragonal *P*4/*ncc*. In all the structures, the XB donor **5** molecules interact with the NARBrs via I···Br XBs. The $Br^-\cdots I-(CF_2)_4-I\cdots Br^-$ halogen-bonded species forms as in the above assemblies. A second NARBr sits in the upper cavity of the XB assembly (Figure 14), in a head-to-tail packing arrangement (Figure 15A,B), rather than in the head-to-head or staggered head-to-head packing arrangement observed in cases discussed above.

DOI: 10.1021/jacs.5b06590
J. Am. Chem. Soc. 2015, 137, 10406−10413

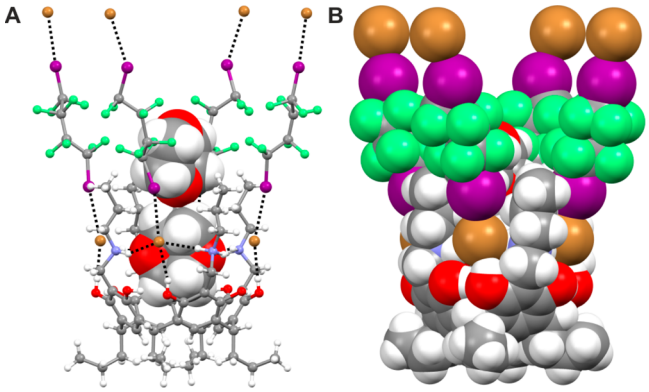

Figure 14. Projection to show the deep cavity cavitands in the assembly of $[(\mathbf{6}_2@\mathbf{3})\cdot\mathbf{5}_2]$ in ball-and-stick model with the with the guest 1,4-dioxane molecule in the cavity in CPK mode (A) and CPK mode for the whole assembly (B).

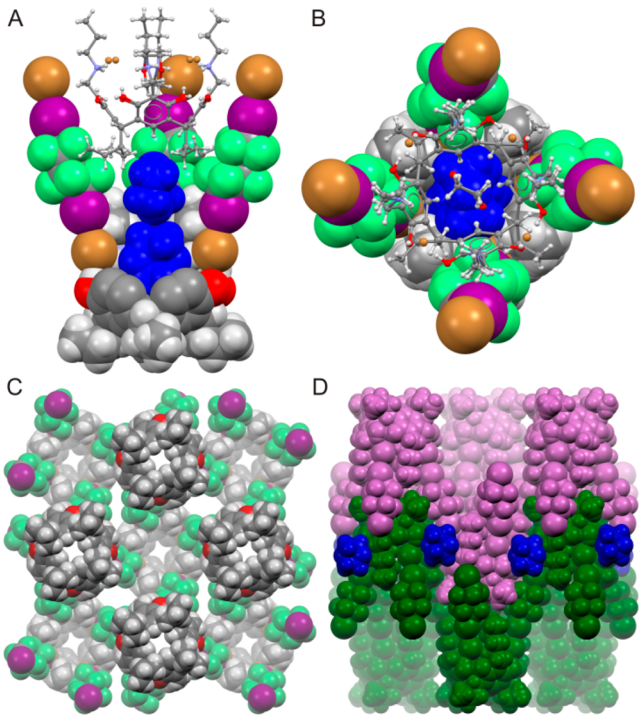

Figure 15. Sliced side (A) and top (B) view of the XB-extended-cavity $[(\mathbf{6}_2@\mathbf{3})\cdot\mathbf{5}_2]$ with two 1,4-dioxane molecules and one resorcinarene host inside. (C) The halogen-bonded layer with peaks and holes; (D) packing to show the fit of the layers (green and violet) with additional 1,4-dioxane molecules (blue) filling in the lattice. The situation in $[(\mathbf{6}_2@\mathbf{3}')\cdot\mathbf{5}_2]$ and $[(\mathbf{6}_2@\mathbf{4})\cdot\mathbf{5}_2]$ is very similar (Figure S10).

Two 1,4-dioxane molecules fill up the deep cavity, and one situates outside the cavity in the cases of **3**. In the case of **4**, no additional outside 1,4-dioxane exits because of the relatively larger cyclohexyl group in the upper rim (Figures S9 and S10). All the guest molecules are disordered due to the high symmetry. For the same reason, the XB donor **5** exhibits disorder over two positions appearing in gauche conformation (Figure 14). Interestingly, the preferable self-inclusion dimeric assembly strongly associated with the pure *N*-propyl NARXs[13,20] is completely overcome by the suitable HB donor 1,4-dioxane and XB donor **5** and superseded by this deep-cavity cavitand architecture.

The four XB donor **5** molecules bonding with each NARBr interact with another four neighboring NARBr molecules along two directions, thus spanning the assemblies in a plane resulting to a sheet with holes and peaks on both sides like an egg-crate (Figure 15C). The peaks of one sheet fit into the holes of the neighbors perfectly (Figure 15D). To reach the most efficient packing, additional 1,4-dixoane molecules are located between the layers to make up the shortness of the upper rim groups which can be clearly seen in Figure 15D, where the additional void-filling 1,4-dioxanes are shown in blue with the two adjacent layers in green and violet, respectively. There are only one-quarter **5** in $[(\mathbf{6}_2@\mathbf{4})\cdot\mathbf{5}_2]$ and two quarters of XB donor **5** in $[(\mathbf{6}_2@\mathbf{3})\cdot\mathbf{5}_2]$ due to the high symmetry. Moreover, because disorder happens to the molecule **5** in all the cases, the observed average Br···I distances are 3.285 and 3.438 Å, with the average R_{XB} ratio of 0.86 and 0.90 in $[(\mathbf{6}_2@\mathbf{3})\cdot\mathbf{5}_2]$ and $[(\mathbf{6}_2@\mathbf{4})\cdot\mathbf{5}_2]$, respectively.

3. CONCLUSION

The present work reports HB and XB working in tandem to successfully form a variety of exotic supramolecular architectures between NARBrs **1**−**4** and 1,4-diiodooctafluorobutane **5** with guests **6** and **7** binding properties. Multiple HB stabilizes the NARBr in a cavitand-like structure. With *N*-benzyl upper rim substituent, four XB donors **5** through eight intermolecular $-CF_2I\cdots Br^-$ XBs connect two NARBrs forming a dumbbell-like dimeric assembly. Single crystal X-ray diffraction study showed the assembly trapping two 1,4-dioxane **6** molecules in each cavity of NARBr. Solution studies showed a dynamic mixture consisting of both 1:1 and 1:2 XB acceptor−XB donor assemblies in solution, which were capable of binding both 1,4-dioxane **6** and *N*-methylacetamide **7** in each resorcinarene cavity. A change from the *N*-benzyl group to the *N*-hexyl group resulted in an XB-induced dimeric pseudocapsular and an XB-induced dimeric capsular assemblies with entrapped 1,4-dioxane molecules in each resorcinarene cavity in the solid state. In the pseudocapsular assembly, each resorcinarene is halogen bonded to only three XB donors **5** with only two of them connecting the pseudocapsule. The third XB donor connects to a different NARBr resulting in a 1D pseudocapsular polymer. In the dimeric capsule, each resorcinarene is halogen bonded to two XB donors **5** connecting the capsule halves. The changes in the electronic environment caused by XB were observed through multiple NMR measurements. A subtle change from the *N*-hexyl group to either the *N*-propyl or *N*-cyclohexyl groups gave XB deep cavity cavitands with interesting packing arrangements leading to a polymeric herringbone arrangement in one direction. In these assemblies, each XB donor **5** molecule interacts with two different hosts in opposite directions leading to a 3D polymeric arrangement resembling an egg-crate-like supramolecular network. In general, solution studies through ^1H, ^{19}F, and ^{13}C NMR confirm the existence of XB in solution with guest binding properties. This work highlights the benefits of HB and XB working in tandem in a cooperative manner to successfully construct exotic functional architectures. The understanding of such processes can help in the design of more complex and functional supramolecular architectures.

■ ASSOCIATED CONTENT

Supporting Information

The Supporting Information is available free of charge on the ACS Publications website at DOI: 10.1021/jacs.5b06590.

DOI: 10.1021/jacs.5b06590
J. Am. Chem. Soc. 2015, 137, 10406−10413

Single crystal X-ray diffraction and NMR spectroscopic data (PDF). CCDC 1417050, 1417051, 1417049, 1417021, 1417020, and 1417052 contain the supplementary crystallographic data for this paper. These data can be obtained free of charge from The Cambridge Crystallographic Data Centre via www.ccdc.cam.ac.uk/data_request/cif.
Characterization data (CIF)
CIF/PLATON report 6@1-5_2 (PDF)
Characterization data (CIF)
CIF/PLATON report 6-MeOH@2.5_1.5(PDF)
Characterization data (CIF)
Characterization data (CIF)
CIF/PLATON report 6@3′-5_2 (PDF)
Characterization data (CIF)
CIF/PLATON report 6@3-5_2 (PDF)
Characterization data (CIF)
CIF/PLATON report 6@4-5_2 (PDF)

AUTHOR INFORMATION

Corresponding Authors

*ngong.k.beyeh@jyu.fi
*kari.t.rissanen@jyu.fi

Notes

The authors declare no competing financial interest.

ACKNOWLEDGMENTS

N.K.B., F.P., and K.R. gratefully acknowledge the Academy of Finland (N.K.B.: grant no. 258653, K.R.,: grant nos. 263256 and 265328) and the University of Jyväskylä for financial support.

REFERENCES

(1) Special issue: 35 Years of Synthetic Anion Receptor Chemistry 1968−2003 Gale, P. A. *Coord. Chem. Rev.* **2003**, *240*, 1.
(2) (a) Park, C. H.; Simmons, H. E. *J. Am. Chem. Soc.* **1968**, *90*, 2431. (b) Graf, E.; Lehn, J. M. *J. Am. Chem. Soc.* **1976**, *98*, 6403. (c) Schmidtchen, F. P. *Angew. Chem., Int. Ed. Engl.* **1977**, *16*, 720. (d) Yang, X.; Knobler, C. B.; Hawthorne, M. F. *Angew. Chem., Int. Ed. Engl.* **1991**, *30*, 1507. (e) Azuma, Y.; Newcomb, M. *Organometallics* **1984**, *3*, 9. (f) Katz, H. E. *Organometallics* **1987**, *6*, 1134. (g) Tamao, K.; Hayashi, T.; Ito, Y. *J. Organomet. Chem.* **1996**, *506*, 85. (h) Aromí, G.; Gamez, P.; Kooijman, H.; Spek, A. L.; Driessen, W. L.; Reedijk, J. *Eur. J. Inorg. Chem.* **2003**, *2003*, 1394.
(3) (a) Desiraju, G. R. *Angew. Chem., Int. Ed. Engl.* **1995**, *34*, 2311. (b) Conn, M. M.; Rebek, J. *Chem. Rev.* **1997**, *97*, 1647.
(4) (a) Desiraju, G. R.; Ho, P. S.; Kloo, L.; Legon, A. C.; Marquardt, R.; Metrangolo, P.; Politzer, P.; Resnati, G.; Rissanen, K. *Pure Appl. Chem.* **2013**, *85*, 1711.
(5) (a) Clark, T.; Hennemann, M.; Murray, J. S.; Politzer, P. *J. Mol. Model.* **2007**, *13*, 291. (b) Politzer, P.; Murray, J. S. *ChemPhysChem* **2013**, *14*, 278.
(6) (a) Chakrabarti, P. *J. Mol. Biol.* **1993**, *234*, 463. (b) Pennington, W. T.; Hanks, T. W.; Arman, H. D. *Halogen Bonding: Fundamentals and Applications* **2008**, *126*, 65. (c) Troff, R. W.; Mäkelä, T.; Topić, F.; Valkonen, A.; Raatikainen, K.; Rissanen, K. *Eur. J. Org. Chem.* **2013**, *2013*, 1617. (d) Fourmigué, M. *Curr. Opin. Solid State Mater. Sci.* **2009**, *13*, 36. (e) Metrangolo, P.; Meyer, F.; Pilati, T.; Resnati, G.; Terraneo, G. *Angew. Chem., Int. Ed.* **2008**, *47*, 6114. (f) Brammer, L.; Minguez Espallargas, G.; Libri, S. *CrystEngComm* **2008**, *10*, 1712. (g) Raatikainen, K.; Rissanen, K. *CrystEngComm* **2011**, *13*, 6972. (h) Tuikka, M.; Niskanen, M.; Hirva, P.; Rissanen, K.; Valkonen, A.; Haukka, M. *Chem. Commun.* **2011**, *47*, 3427. (i) Raatikainen, K.; Rissanen, K. *Chem. Sci.* **2012**, *3*, 1235.
(7) (a) Sessler, J. L.; Sansom, P. I.; Andrievsky, A. *Supramolecular Chemistry of Anions*; Bianchi, A., Bowman-James, K., García-Espana, E., Eds.; Wiley-VCH: New York, 1997; pp 1−480. (b) Beer, P. D.; Gale, P. A. *Angew. Chem., Int. Ed.* **2001**, *40*, 486.
(8) (a) Metrangolo, P.; Pilati, T.; Terraneo, G.; Biella, S.; Resnati, G. *CrystEngComm* **2009**, *11*, 1187. (b) Cavallo, G.; Metrangolo, P.; Pilati, T.; Resnati, G.; Sansoterra, M.; Terraneo, G. *Chem. Soc. Rev.* **2010**, *39*, 3772.
(9) Chudzinski, M. G.; McClary, C. A.; Taylor, M. S. *J. Am. Chem. Soc.* **2011**, *133*, 10559.
(10) (a) Weiss, R.; Rechinger, M.; Hampel, F.; Wolski, A. *Angew. Chem., Int. Ed. Engl.* **1995**, *34*, 441. (b) Ghassemzadeh, M.; Harms, K.; Dehnicke, K. *Chem. Ber.* **1996**, *129*, 115. (c) Yamamoto, H.; Yamaura, J.; Kato, R. *J. Mater. Chem.* **1998**, *8*, 15. (d) Yamamoto, H. M.; Maeda, R.; Yamaura, J.-I.; Kato, R. *J. Mater. Chem.* **2001**, *11*, 1034. (e) Barres, A.-L.; El-Ghayoury, A.; Zorina, L. V.; Canadell, E.; Auban-Senzier, P.; Batail, P. *Chem. Commun.* **2008**, 2194.
(11) (a) Yamamoto, H. M.; Kato, R. *Chem. Lett.* **2000**, *29*, 970. (b) Yamamoto, H. M.; Kosaka, Y.; Maeda, R.; Yamaura, J.; Nakao, A.; Nakamura, T.; Kato, R. *ACS Nano* **2008**, *2*, 143. (c) Lieffrig, J.; Yamamoto, H. M.; Kusamoto, T.; Cui, H.; Jeannin, O.; Fourmigué, M.; Kato, R. *Cryst. Growth Des.* **2011**, *11*, 4267. (d) Metrangolo, P.; Meyer, F.; Pilati, T.; Resnati, G.; Terraneo, G. *Chem. Commun.* **2008**, 1635. (e) Triguero, S.; Llusar, R.; Polo, V.; Fourmigué, M. *Cryst. Growth Des.* **2008**, *8*, 2241.
(12) Lieffrig, J.; Jeannin, O.; Fourmigué, M. *J. Am. Chem. Soc.* **2013**, *135*, 6200.
(13) (a) Airola, K.; Böhmer, V.; Paulus, E. F.; Rissanen, K.; Schmidt, C.; Thondorf, I.; Vogt, W. *Tetrahedron* **1997**, *53*, 10709. (b) Shivanyuk, A.; Spaniol, T. P.; Rissanen, K.; Kolehmainen, E.; Böhmer, V. *Angew. Chem., Int. Ed.* **2000**, *39*, 3497. (c) Beyeh, N. K.; Cetina, M.; Löfman, M.; Luostarinen, M.; Shivanyuk, A.; Rissanen, K. *Supramol. Chem.* **2010**, *22*, 737. (d) Beyeh, N. K.; Cetina, M.; Rissanen, K. *Cryst. Growth Des.* **2012**, *12*, 4919.
(14) (a) Beyeh, N. K.; Cetina, M.; Rissanen, K. *Chem. Commun.* **2014**, *50*, 1959. (b) Beyeh, N. K.; Valkonen, A.; Bhowmik, S.; Pan, F.; Rissanen, K. *Org. Chem. Front.* **2015**, *2*, 340.
(15) Mecozzi, S.; Rebek, J. *Chem. - Eur. J.* **1998**, *4*, 1016.
(16) Beyeh, N. K.; Pan, F.; Rissanen, K. *Angew. Chem., Int. Ed.* **2015**, *54*, 7303.
(17) (a) Lehn, J.-M. *Pure Appl. Chem.* **1994**, *66*, 1961. (b) Braga, D. *Chem. Commun.* **2003**, 2751.
(18) (a) Bertrán, J. F.; Rodríguez, M. *Org. Magn. Reson.* **1980**, *14*, 244. (b) Erdelyi, M. *Chem. Soc. Rev.* **2012**, *41*, 3547. (c) Sarwar, M. G.; Ajami, D.; Theodorakopoulos, G.; Petsalakis, I. D.; Rebek, J. *J. Am. Chem. Soc.* **2013**, *135*, 13672. (d) Metrangolo, P.; Neukirch, H.; Pilati, T.; Resnati, G. *Acc. Chem. Res.* **2005**, *38*, 386. (e) *Halogen Bonding: Fundamentals and Applications*; Metrangolo, P., Resnati, G., Eds.; Springer-Verlag: Berlin, 2008; pp 1.
(19) Aakeröy, C. B.; Rajbanshi, A.; Metrangolo, P.; Resnati, G.; Parisi, M. F.; Desper, J.; Pilati, T. *CrystEngComm* **2012**, *14*, 6366.
(20) Dumele, O.; Trapp, N.; Diederich, F. *Angew. Chem., Int. Ed.* **2015**, DOI: 10.1002/anie.201502960.
(21) (a) Beyeh, N. K.; Ala-Korpi, A.; Cetina, M.; Valkonen, A.; Rissanen, K. *Chem. - Eur. J.* **2014**, *20*, 15144. (b) Beyeh, N. K.; Ala-Korpi, A.; Pan, F.; Jo, H.; Anslyn, E. V.; Rissanen, K. *Chem. - Eur. J.* **2015**, *21*, 9556−9562.
(22) (a) Hirose, K. In *Analytical Methods in Supramolecular Chemistry*; Wiley-VCH Verlag GmbH & Co. KGaA: Weinheim, 2012; pp 27. (b) Hirose, K. *J. Inclusion Phenom. Mol. Recognit. Chem.* **2001**, *39*, 193. (c) Thordarson, P. *Chem. Soc. Rev.* **2011**, *40*, 1305.
(23) Allen, F. H. *Acta Crystallogr., Sect. B: Struct. Sci.* **2002**, *58*, 380.
(24) (a) Lommerse, J. P. M.; Stone, A. J.; Taylor, R.; Allen, F. H. *J. Am. Chem. Soc.* **1996**, *118*, 3108. (b) Brammer, L.; Bruton, E. A.; Sherwood, P. *Cryst. Growth Des.* **2001**, *1*, 277. (c) Zordan, F.; Brammer; Sherwood, L. P. *J. Am. Chem. Soc.* **2005**, *127*, 5979.
(25) Baker, R. J.; Colavita, P. E.; Murphy, D. M.; Platts, J. A.; Wallis, J. D. *J. Phys. Chem. A* **2012**, *116*, 1435.

DOI: 10.1021/jacs.5b06590
J. Am. Chem. Soc. 2015, 137, 10406−10413